Bioorganic & Medicinal Chemistry xxx (xxxx) xxx–xxx

Contents lists available at ScienceDirect

Bioorganic & Medicinal Chemistry

journal homepage: www.elsevier.com/locate/bmc

Kinase inhibitions in pyrido[4,3-*h*] and [3,4-*g*]quinazolines: Synthesis, SAR and molecular modeling studies

Wael Zeinyeh[a], Yannick J. Esvan[a], Béatrice Josselin[b], Blandine Baratte[b], Stéphane Bach[b], Lionel Nauton[a], Vincent Théry[a], Sandrine Ruchaud[b], Fabrice Anizon[a], Francis Giraud[a,*], Pascale Moreau[a,*]

[a] Université Clermont Auvergne, CNRS, SIGMA Clermont, ICCF, F-63000 Clermont-Ferrand, France
[b] Sorbonne Université, CNRS, Plateforme de criblage KISSf (Kinase Inhibitor Specialized Screening facility), Protein Phosphorylation and Human Diseases Unit, Station Biologique, Place Georges Teissier, F-29688 Roscoff, France

ARTICLE INFO

Keywords:
Pyrido[3,4-*g*]quinazolines
Pyrido[4,3-*h*]quinazoline
Protein kinase inhibition
CLK1

ABSTRACT

New pyrido[3,4-*g*]quinazoline derivatives were prepared and evaluated for their inhibitory potency toward 5 protein kinases (CLK1, DYRK1A, GSK3, CDK5, CK1). A related pyrido[4,3-*h*]quinazoline scaffold with an angular structure was also synthesized and its potency against the same protein kinase panel was compared to the analogous pyrido[3,4-*g*]quinazoline. Best results were obtained for 10-nitropyrido[3,4-*g*]quinazoline **4** toward CLK1 with nanomolar activities.

1. Introduction

CLK1 and DYRK1A are serine-threonine protein kinase members of the CMGC family. CLK1 and DYRK1A are implicated in pre-mRNA splicing regulation and, in this context, phosphorylate various serine/arginine-rich proteins. Moreover, DYRK1A and CLK1 are over-expressed in certain types of cancer. Therefore both protein kinases are involved in numerous signalization pathways implicated in various diseases such as cancer or neurodegenerative disorders.[1–3] These two protein kinases constitute relevant targets for the development of new cellular tools and/or therapies. Therefore, the development of new small molecules able to modulate their activity is of high interest. As part of our research program dedicated to the discovery of new heteroaromatic compounds exhibiting protein kinase inhibitory potencies, we recently reported the synthesis of pyrido[3,4-*g*]quinazolines with interesting activities toward CLK1 (cdc2-like kinase 1)/DYRK1A (dual specificity tyrosine-phosphorylation-regulated kinase 1A) or CDK5 (cyclin dependent kinase 5)/GSK3 (glycogen synthase kinase 3), depending on the heteroaromatic scaffold substitution (Fig. 1). Previous structure-activity relationship studies (SAR) undertaken on this scaffold demonstrated that the aminopyrimidine and the pyridine parts were essential to the interactions within the ATP-binding site of the targeted kinases.[4–6] Moreover, we reported that no substitution at the 5-position led to potent CLK1/DYRK1A inhibitions. In contrast, the substitution at the 5-position by alkyl/aryl groups impaired CLK1/DYRK1A inhibition leading to improved potencies toward CDK5/GSK3.[5] In addition, in this series, the presence of a nitro group at the 10-position could lead to a better selectivity profile for CLK1 over DYRK1A while a 10-amino substitution could achieve a better activity toward DYRK1A compared to CLK1.[4,6] Recently, we demonstrated that the incorporation at the 2-position of aminoethylamino or aminopropylamino substituents did not cause major steric hindrance issues and therefore could lead to potent CLK1 and/or DYRK1A inhibitors (Fig. 1). To enlarge the SAR studies performed around this scaffold, we describe herein the preparation of new aminoalkylamino/aminoalkylimino derivatives bearing shortened and/or rigidified groups at the 2-position (Fig. 1). In addition, we continued to explore the chemical space in the pyridoquinazoline series by preparing an angular analogue of the linear pyrido[3,4-*g*]quinazoline scaffold. Thus, pyrido[4,3-*h*]quinazolin-2-amine **11** (Fig. 1) was prepared to measure the impact of this structural change on kinase inhibition.

The first 10-nitropyrido[3,4-*g*]quinazoline series was prepared in 11 steps from commercially available 2-chloro-4-nitrobenzoic acid.[4,5] The formation of the aminopyrimidine part is based on the condensation of a guanidinium salt with key 6-chloro-5-nitroisoquinoline-7-carbaldehyde intermediate **A** (Scheme 1). As recently reported, this strategy was employed to generate *N*-2 substituted derivatives, bearing NO_2 or NH_2 groups at the 10-position (compounds **B**) by reaction of aminoethyl- or aminopropylguanidinium salts with **A** (Scheme 1).[6] In this work we report the preparation of new *N*-2 substituted analogues (compounds **C**)

* Corresponding authors.
E-mail addresses: francis.giraud@uca.fr (F. Giraud), pascale.moreau@uca.fr (P. Moreau).

https://doi.org/10.1016/j.bmc.2019.04.005
Received 25 February 2019; Received in revised form 29 March 2019; Accepted 3 April 2019

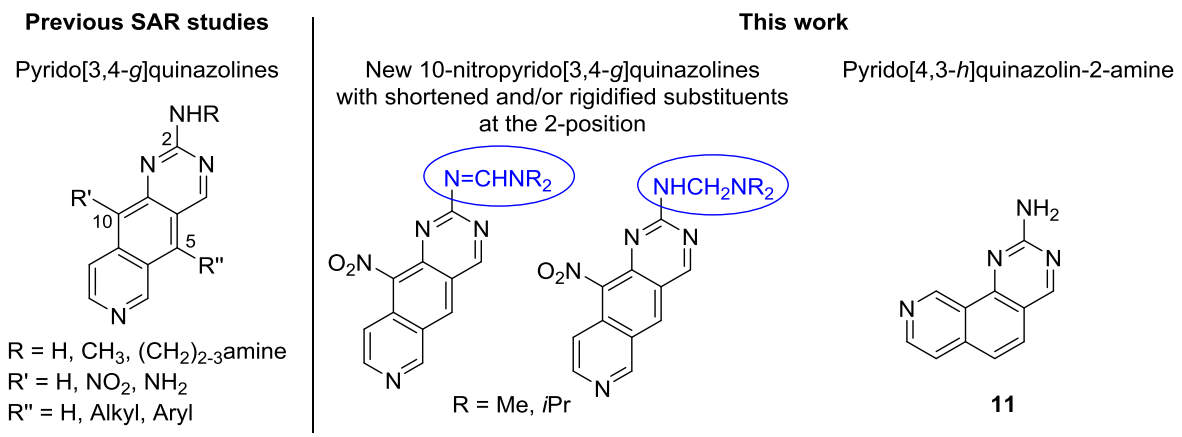

Fig. 1. Chemical structures of pyrido[3,4-*g*]quinazolines and pyrido[4,3-*h*]quinazolin-2-amine. Previous SAR studies and this work.

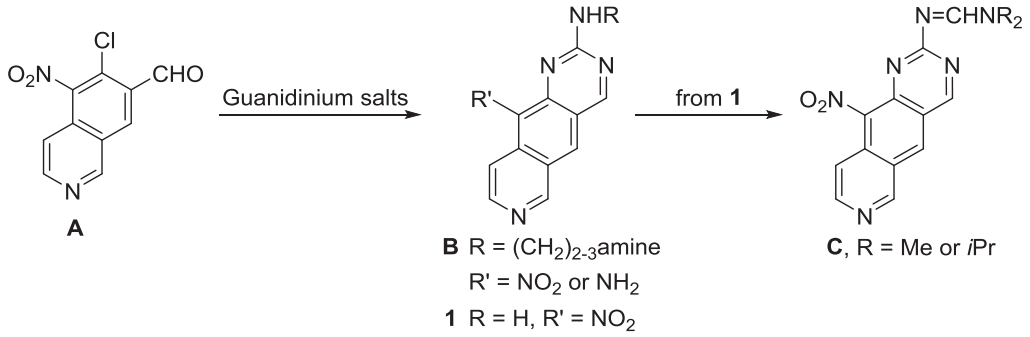

Scheme 1. Synthetic pathways leading to new pyrido[3,4-*g*]quinazolines **C** series.

directly from corresponding aminopyrimidine **1** (Scheme 1).

In addition to this SAR study around the pyrido[3,4-*g*]quinazoline scaffold, we also prepared a regioisomeric analogue with an angular pyrido[4,3-*h*]quinazoline structure. This was carried out from compound **D** (Scheme 2) which was obtained as a minor iodination side-product during the synthesis of compound **A**[4] (Scheme 1) from 2-chloro-4-nitrobenzoic acid (Scheme 2).

Finally, the activity of new synthesized compounds was evaluated toward a panel of 5 protein kinases (CLK1, DYRK1A, GSK3, CDK5, CK1). This panel was chosen on the basis of previous results (CLK1, DYRK1A, GSK3, CDK5)[4–6] and of known kinase cross-inhibitions due to the ATP-binding site kinase homology (CK1).[7]

2. Results and discussion

2.1. Chemistry

Diversely substituted pyrido[3,4-*g*]quinazolines were prepared from known compound **1**.[4] Compound **2** was obtained in 97% yield under Vilsmeier conditions using phosphorous oxychloride and DMF (Scheme 3).[8–10]

Isopropyl analogue **3** was prepared similarly by reaction between **1** and oxalyl chloride/diisopropylformamide in dichloromethane (Scheme 3).[11] Our first attempts to reduce both amidine moiety and nitro group of compounds **2** and **3** using catalytic hydrogenation (H_2, Pd/C, CH_2Cl_2, MeOH) failed. Therefore, we performed the reduction of the amidine part in the presence of $NaBH_4$ in MeOH leading to compounds **4** and **5** in moderate yields.[12] Despite numerous efforts, we never managed to get the corresponding 10-amino analogues of compounds **2–5**. Indeed, due to rapid degradation processes, all reduction attempts led to the formation of complex reaction mixtures.

The preparation of pyrido[4,3-*h*]quinazolin-2-amine **11** started from ethyl 4-amino-2-chlorobenzoate **6**.[4] The product of the first iodination step (I_2, Ag_2SO_4, EtOH), containing minor regioisomer **D** (Scheme 2) was engaged in a 3-steps sequence starting by a CuCN-mediated cyanation before iodination using a Sandmeyer type reaction and reduction (Scheme 4). Minor regioisomer **7** was isolated in 7% overall yield. After Sonogashira coupling of **7** with TMS-acetylene to give **8**, isoquinoline **9** was formed by reaction with ammonia in methanol under microwave irradiation. Oxidation of **9** led to chloroaldehyde **10** that was reacted with guanidine carbonate under microwave irradiation to give product **11**.

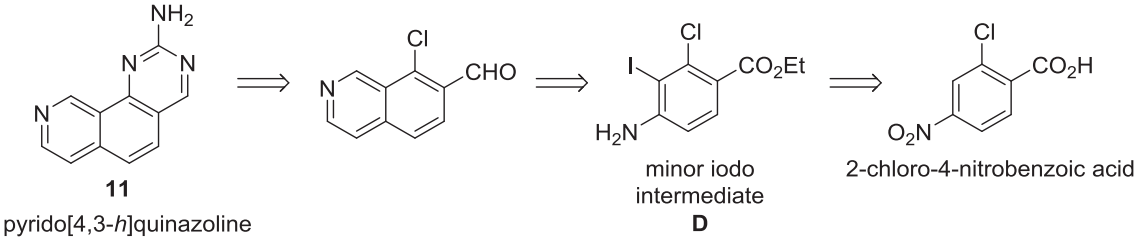

Scheme 2. Retrosynthetic pathway leading to angular pyrido[4,3-*h*]quinazoline analogue **11**.

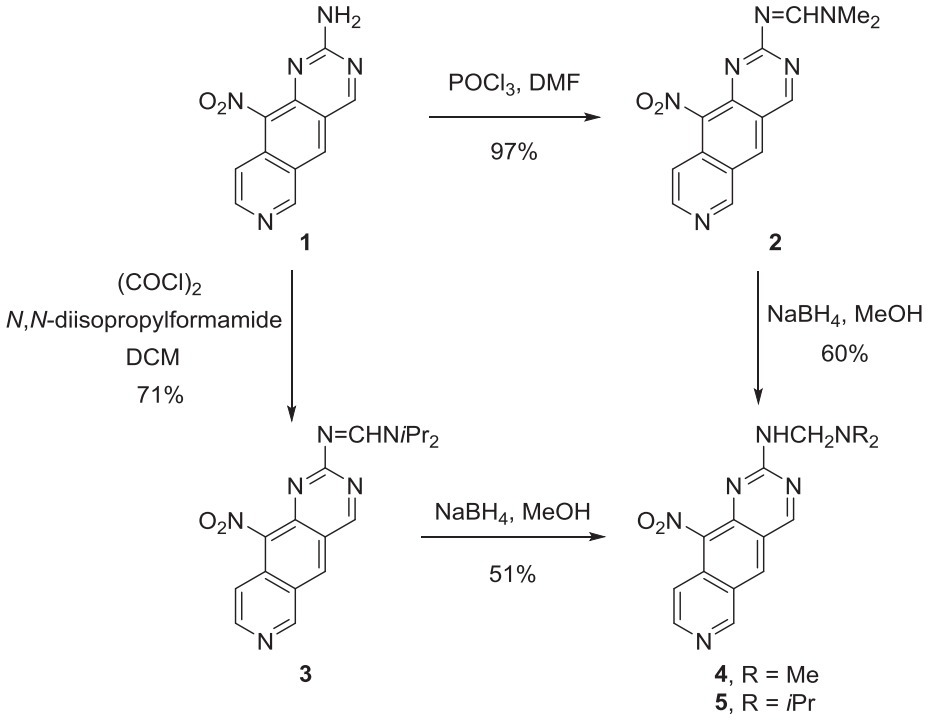

Scheme 3. Preparation of 10-nitropyrido[3,4-*g*]quinazolines **2–5**.

2.2. Kinase inhibition evaluation

Compounds **2–5** and **11** were evaluated toward a panel of 5 protein kinases CLK1, DYRK1A, CDK5/p25, GSK-3α/β and CK1δ/ε. The results are expressed as % of residual kinase activities at 10 μM or 1 μM compound concentration. Except for **11** presenting a new scaffold, IC_{50} values were determined only when % of residual kinase activity was ≤25% at 1 μM. As shown in Table 1, all compounds, including the angular analogue **11**, inhibited CLK1 more than, or around 50% at 1 μM, indicating IC_{50} values in the micro/submicromolar range. Compared to CLK1, compounds **2–4** were less active toward CDK5, GSK3 and CK1 with an important decrease of inhibition at 1 μM. In summary, most inhibited kinases were CLK1 > DYRK1A/GSK3 > CDK5/CK1 with 2-dimethylaminomethylamino derivative **4** being the most potent of the series with IC_{50} value of 87 nM against CLK1. With the exception of CK1, compound **4** exhibited similar in vitro kinase inhibitory potencies compared to the reference of the nitro series (Compound **1**, R = H, R′ = NO_2, R″ = H, Fig. 1). However, the tertiary amino group at the 2-position could advantageously be converted into the corresponding ammonium salt, thus achieving an improved solubility and a better pharmacokinetic profile.

Compound **11**, first analogue of the angular series, exhibited micromolar potencies toward CLK1 and DYRK1A. In comparison, the linear pyrido[3,4-*g*]quinazolin-2-amine analogue (R = R′ = R″ = H, Fig. 1) was more active toward CLK1 and DYRK1A with submicromolar activities (CLK1 IC_{50} value = 0.19 μM, and DYRK1A IC_{50} value = 0.18 μM).[4] Therefore, in order to get insights for further optimization of the kinase inhibitory potential in this new series, we performed molecular modeling studies to determine its plausible binding mode within CLK1 ATP-binding pocket.

2.3. Molecular modeling experiments

The docking experiments were performed using a CLK1 model

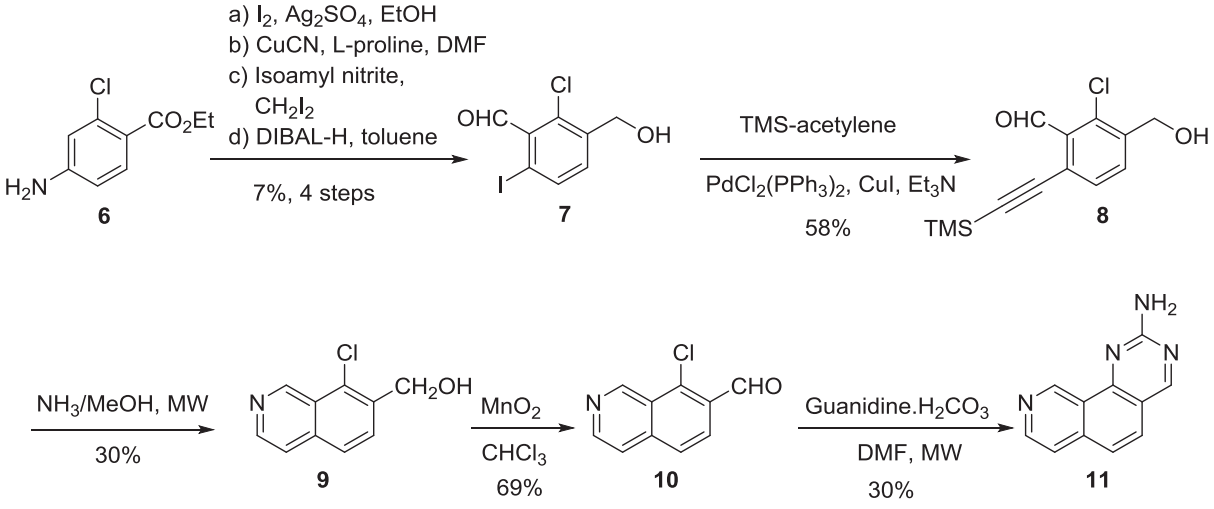

Scheme 4. Synthesis of pyrido[4,3-*h*]quinazolin-2-amine **11**.

Table 1
Kinase inhibitory potencies of reference compound **1** in the nitro series (R = H, R′ = NO_2, R″ = H, Fig. 1) and new analogues **2–5**, **11**.

Cpds	Kinase inhibitory potencies									
	CLK1		DYRK1A		CDK5		GSK3		CK1	
	10 µM	1 µM	10 µM	1 µM	10 µM	1 µM	10 µM	1 µM	10 µM	1 µM
1	2 (0.069 µM)[4]	6	5 (0.62 µM)[4]	36	56 (> 10 µM)[4]	88	25 (2.2 µM)[4]	74	9 (0.78 µM)[4]	41
2	3	33	31	100	59	94	30	86	53	100
3	1	53	46	95	45	100	15	73	60	96
4	6 (0.087 µM)	13	4	39	41	99	15	73	38	100
5	5	44	46	69	61	99	1	53	38	74
11	9 (1.48 µM)	48	25 (2.18 µM)	71	63	100	75	98	22	64

% of Residual kinase activities and IC_{50} values in brackets. Assays performed using a ^{32}P radioassay (method A), except for the determination of compound **11** IC_{50} values that was carried out using the ADP-Glo assay (method B). Compound **1** IC_{50} values against CLK1, DYRK1A, CDK5, GSK3 and CK1 were previously reported.[4] Kinase activities were assayed in triplicate. Typically, the standard deviation of single data points was below 10%.

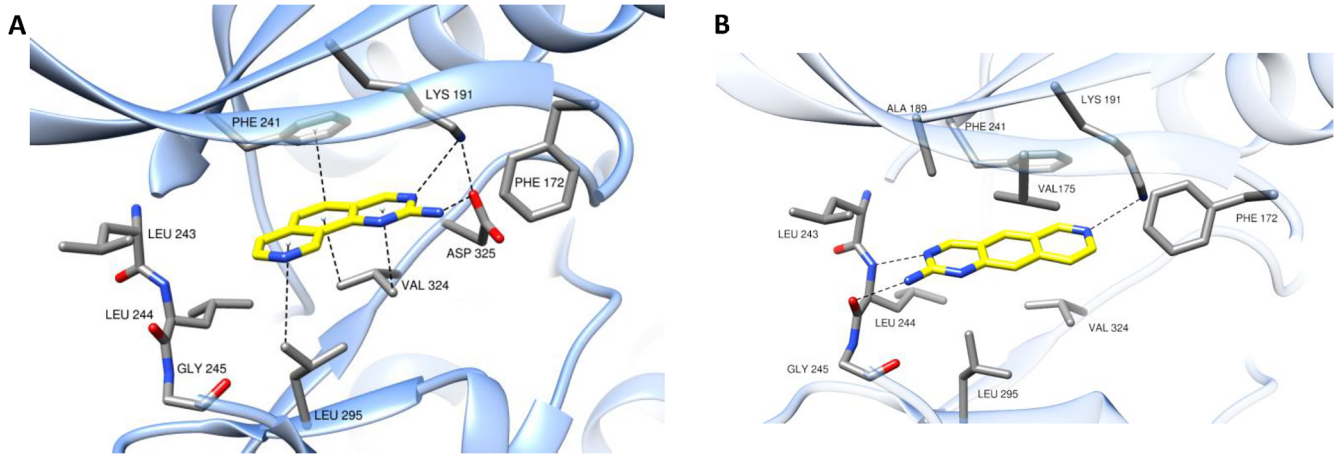

Fig. 2. A) Plausible binding mode of **11** within CLK1 ATP-binding site. B) Binding mode of linear pyrido[3,4-*g*]quinazolin-2-amine analogue solved by X-ray crystallography (PDB code 5J1W).[4] The images were produced using UCSF Chimera.[16]

generated from 6FT8 structure available in the Protein Data Bank[13] using AutoDock Vina.[14,15] As shown in Fig. 2A, compound **11** does not establish H-bond within the hinge, but is inserted in CLK1 ATP-binding pocket with 2 hydrogen bonds established between the aminopyrimidine part and Asp325 and Lys191 residues. In addition, hydrophobic interactions involving Leu295, Val324 and Phe241 residues participated in the binding of **11** to CLK1.

Contrarily to what was observed for the linear pyrido[3,4-*g*]quinazolin-2-amine (Fig. 2B) in which both aminopyrimidine and pyridine parts were H-bonded to the ATP-binding pocket (hinge Leu244 and Lys191 residues) the angular structure of **11** does not allow H-bonding of the pyridine part within CLK1 active site. This could explain the lower activity of **11** in comparison to best active pyrido[3,4-*g*]quinazolines from the linear series.[4,6] These results indicated that the biological profile of this new series could be improved by modification of the pyridine part in order to reinforce the interaction with targeted kinase.

3. Conclusion

The synthesis of new 2-aminoalkylamino substituted 10-nitropyrido[3,4-*g*]quinazolines was achieved from the corresponding 10-nitropyrido[3,4-*g*]quinazolin-2-amine **1**. Compound **4** was the most active of the series with nanomolar activities toward CLK1 which is an attractive target for the development of new therapies in various therapeutical areas such as cancer and neurodegenerative disorders. The biological potential of compound **4**, particularly its cellular effects, will be evaluated in more details. Furthermore, we described the first synthesis of pyrido[4,3-*h*]quinazolin-2-amine **11**. Its kinase inhibitory potential was inferior to the one of the 10-nitropyrido[3,4-*g*]quinazolines. However, the study of **11** binding mode within CLK1 binding site gave valuable information for future structure-activity relationship studies in this angular series, in order to reach better kinase inhibitory potencies.

4. Experimental

4.1. Chemistry

4.1.1. General

Starting materials were obtained from commercial suppliers and used without further purification. Solvents were distilled before use. IR spectra were recorded on a Shimadzu FTIR-8400S spectrometer ($\bar{\nu}$ in cm^{-1}). NMR spectra, performed on a Bruker AVANCE 400 (^1H: 400 MHz, ^{13}C: 100 MHz), are reported in ppm using the solvent residual peak as an internal standard; the following abbreviations are used: singlet (s), doublet (d), triplet (t), heptuplet (hept), doublet of doublet (dd), multiplet (m), broad signal (br s). High resolution mass spectra (ESI+) were determined on a high-resolution Waters Micro Q-Tof apparatus (UCA-Partner, Université Clermont Auvergne, Clermont-Ferrand, France). Chromatographic purifications were performed by column chromatography using 40–63 µm silica gel. Experiments under

microwave irradiation were performed using a CEM Discover Benchmate apparatus. Reactions were monitored by TLC using fluorescent silica gel plates (60 F254 from Merck). Melting points were measured on a Stuart SMP3 apparatus and are uncorrected. The purity of tested compounds **2–5** and **11** was determined by HPLC analysis using a Hitachi liquid chromatograph (Oven 5310, 30 °C; Pump 5160; DAD detector 5430) and a C18 Acclaim column (4.6 mm × 250 mm, 5 µm, 120 Å). Detection wavelength was 240 nm (compound **11**) or 280 nm (compounds **2–5**), and flow rate 0.5 mL/min. Gradient elution used (A) water/0.1% TFA; (B) acetonitrile: 95:5 A/B for 5 min then 95:5 A/B to 5:95 A/B in 25 min and then 5:95 A/B for 10 min.

4.1.2. *N,N-Dimethyl-N′-(10-nitropyrido[3,4-g]quinazolin-2-yl) formimidamide (**2**)*

Phosphorus oxychloride (116 µL, 1.244 mmol, 3.0 eq.) was added dropwise to 3.5 mL of anhydrous DMF at 0 °C under argon. Stirring at 0 °C was continued for 45 min before dropwise addition of a solution of compound **1** (100 mg, 0.415 mmol) in 6 mL of DMF. After 1 h at 0 °C, the reaction was hydrolysed by addition of 4 mL of saturated $NaHCO_3$ solution at this temperature. Water was added and the solution was extracted with DCM. The organic layer was dried over $MgSO_4$ and concentrated under reduced pressure. Residue was purified by flash chromatography using DCM/Acetone 1:1 and finally 1:2 as eluant, yielding the pure compound **2** (120 mg, 0.405 mmol, 97%) as a yellow powder. TLC $R_f = 0.30$ (CH_2Cl_2/acetone 1:1). mp: 184–185 °C. IR (ATR): 2922, 1624, 1563, 1465, 1324 cm^{-1}. ^1H NMR (400 MHz, DMSO-d_6): 3.16 (3H, s), 3.26 (3H, s), 7.65 (1H, d, J = 6.4 Hz), 8.63 (1H, d, J = 6.0 Hz), 8.95 (1H, s), 9.17 (1H, d, J = 0.8 Hz), 9.65 (1H, d, J = 0.8 Hz), 9.78 (1H, s). ^{13}C NMR (100 MHz, DMSO-d_6): 35.2, 41.2 (CH_3), 112.5, 134.0, 146.1, 155.3, 160.2, 164.9 (CH_{arom}), 120.6, 124.0, 128.0, 138.1, 141.1, 161.3 (C_{arom}). HRMS (ESI+) calcd for $C_{14}H_{13}N_6O_2$ $(M+H)^+$ 297.1100, found 297.1098. HPLC: purity > 95%, t_R = 18.8 min.

4.1.3. *N,N-Diisopropyl-N′-(10-nitropyrido[3,4-g]quinazolin-2-yl) formimidamide (**3**)*

To a solution of *N,N*-diisopropylformamide (150 µL, 1.03 mmol, 24.9 eq.) in 1 mL of anhydrous DCM at 0 °C under argon was added dropwise oxalyl chloride (90 µL, 1.03 mmol, 24.9 eq.). The solution was allowed to reach room temperature for 30 min, the obtained yellow suspension was cooled again to 0 °C. Compound **1** (10.0 mg, 0.0415 mmol) was added in one portion as a solid. Reaction mixture was maintained for 20 min at room temperature; an orange solution was observed. DCM was added and the solution poured on 10 mL of aqueous K_2CO_3 solution (10%). The organic layer was washed with water, dried over $MgSO_4$ and concentrated under reduced pressure. Residue was purified by flash chromatography using DCM/acetone 9:1 and finally 8:2 as eluant, yielding the pure compound **3** (10 mg, 0.028 mmol, 71%) as an orange powder. TLC $R_f = 0.20$ (CH_2Cl_2/Acetone 8:2). mp: 218–219 °C. IR (ATR): 3027–2767, 1617, 1587, 1561, 1527, 1291 cm^{-1}. ^1H NMR (400 MHz, DMSO-d_6): 1.29 (6H, d, J = 7.2 Hz), 1.34 (6H, d, J = 6.8 Hz), 3.86–4.01 (1H, m), 4.84–4.97 (1H, m), 7.66 (1H, d, J = 6.4 Hz), 8.63 (1H, d, J = 6.0 Hz), 9.10 (1H, s), 9.18 (1H, s), 9.66 (1H, s), 9.78 (1H, s). ^{13}C NMR (100 MHz, DMSO-d_6): 19.5, 23.7 (2 × 2 CH_3), 47.1, 47.4 (CH), 112.5, 134.1, 146.1, 155.3, 157.6, 164.9 (CH_{arom}), 120.6, 123.1, 128.0, 138.1, 141.1, 164.7 (C_{arom}). HRMS (ESI+) calcd for $C_{18}H_{21}N_6O_2$ $(M+H)^+$ 353.1726, found 353.1715. HPLC: purity > 96%, t_R = 21.5 min.

4.1.4. *N,N-Dimethyl-N′-(10-nitropyrido[3,4-g]quinazolin-2-yl) methanediamine (**4**)*

To a solution of compound **2** (20 mg, 0.067 mmol) in 1 mL of anhydrous MeOH under argon was added sodium borohydride (5 mg, 0.132 mmol, 2.0 eq.) at room temperature. After 1 h of reaction, additional 2.5 mg of $NaBH_4$ were added and reaction was left to continue for 30 min. Water was added and the solution was extracted with DCM. The organic layer was dried over $MgSO_4$ and concentrated under reduced pressure. Residue was purified by preparative TLC using DCM/Acetone 2:3 as eluant, yielding the pure compound **4** (12 mg, 0.040 mmol, 60%) as a yellow powder. TLC $R_f = 0.20$ (CH_2Cl_2/MeOH 96:4). mp: 190–191 °C. IR (ATR): 3314–2315, 1630, 1517, 1415, 1335, 1270 cm^{-1}. ^1H NMR (400 MHz, DMSO-d_6): 2.99 (3H, s), 3.11 (3H, s), 4.72 (2H, s), 7.22 (1H, d, J = 5.6 Hz), 7.73 (1H, br s), 7.75 (1H, s), 8.36 (1H, d, J = 6.0 Hz), 8.48 (1H, s), 9.03 (1H, s). ^{13}C NMR (100 MHz, DMSO-d_6): 34.7, 40.9 (CH_3), 42.4 (CH_2), 112.1, 125.4, 144.9, 151.0, 158.3 (CH_{arom}), 122.6, 125.5, 128.1, 138.1, 141.8, 161.1 (C_{arom}). HRMS (ESI+) calcd for $C_{14}H_{15}N_6O_2$ $(M+H)^+$ 299.1256, found 299.1271. HPLC: purity > 95%, t_R = 18.6 min.

4.1.5. *N,N-Diisopropyl-N′-(10-nitropyrido[3,4-g]quinazolin-2-yl) methanediamine (**5**)*

Following the same procedure as described for compound **4**, starting from 25 mg (0.071 mmol) of compound **3** dissolved in 1 mL MeOH under argon at 0 °C. $NaBH_4$ (6 mg, 0.159 mmol, 2.2 eq.) was added and the solution stirred at room temperature for 2 h. Additional 6 mg of $NaBH_4$ were added and stirring continued for 2 h. The solution was extracted with DCM. The organic layer was dried over $MgSO_4$ and concentrated under reduced pressure. Residue was purified by column chromatography using DCM/MeOH 97:3 as eluant, yielding residual starting material **3** (8 mg, 0.023 mmol). Changing to DCM/MeOH 95:5 afforded pure compound **5** as an oily residue which was subsequently triturated in cyclohexane to give a yellow powder (13 mg, 0.036 mmol, 51%). TLC $R_f = 0.65$ (CH_2Cl_2/MeOH 96:4). mp: 131–132 °C. IR (ATR): 3045–2853, 1592, 1561, 1504, 1275, 1108 cm^{-1}. ^1H NMR (400 MHz, DMSO-d_6): 1.22 (6H, d, J = 6.8 Hz), 1.24 (6H, d, J = 6.8 Hz), 3.79 (1H, hept, J = 6.8 Hz), 4.62 (1H, hept, J = 6.8 Hz), 4.72 (2H, br s), 7.24 (1H, d, J = 6.0 Hz), 7.75 (2H, br s), 8.36 (1H, d, J = 6.0 Hz), 8.81 (1H, s,), 9.02 (1H, s). ^{13}C NMR (100 MHz, DMSO-d_6): 19.4, 23.6 (2 × 2CH_3), 42.4 (CH_2), 46.5 (2CH), 112.2, 125.5, 144.9, 151.0, 156.0 (CH_{arom}), 122.6, 125.7 (2C), 128.1, 141.9, 161.4 (C_{arom}). HRMS (ESI+) calcd for $C_{18}H_{23}N_6O_2$ $(M+H)^+$ 355.1882, found 355.1859. HPLC: purity > 90%, t_R = 21.6 min.

4.1.6. *2-Chloro-3-(hydroxymethyl)-6-iodobenzaldehyde (**7**)*

Compound **7** was prepared using a 4-step procedure, similar to the one described in the literature, without separating the mixture of regioisomers produced step A until step D.[4] Only chemical quantities used and protocol changes are described below.

4.1.6.1. Step A. Compound **6** (5.00 g, 25.05 mmol), anhydrous ethanol (250 mL), silver sulfate (7.81 g, 25.05 mmol), iodine (6.36 g, 25.05 mmol). 45 min (0 °C) and additional 90 min (room temperature).

Mixture (7.28 g) of ethyl 4-amino-2-chloro-5-iodobenzoate (major) and ethyl 4-amino-2-chloro-3-iodobenzoate (minor) was directly engaged in the next step.

4.1.6.2. Step B. Mixture from step A (7.28 g), *N,N*-dimethylformamide (21 mL), copper(I) cyanide (4.00 g, 44.66 mmol), L-proline (2.57 g, 22.37 mmol). 60 h (80 °C).

Mixture (4.67 g) of ethyl 4-amino-2-chloro-5-cyanobenzoate (major) and ethyl 4-amino-2-chloro-3-cyanobenzoate (minor) was obtained and directly engaged in the next step.

4.1.6.3. Step C. Mixture from step B (4.67 g), diiodomethane (15 mL), isoamyl nitrite (5.23 mL, 39.10 mmol). 45 min (room temperature), 80 °C (3 h).

Residue was purified by column chromatography (EtOAc/cyclohexane 1:99 to 3:97). Combined fractions were triturated in a minimal amount of pentane to give a mixture (5.58 g) of ethyl 2-chloro-5-cyano-4-iodobenzoate (major) and ethyl 2-chloro-3-cyano-4-iodobenzoate (minor).

4.1.6.4. Step D. Mixture from step C (5.58 g), toluene (95 mL), 1.2 M solution of DIBAL-H in toluene (44.4 mL, 53.25 mmol). 1 h 30 min (−78 °C) and additional 1 h 30 (room temperature). The solution was extracted with EtOAc, the organic layers were washed with brine, dried over $MgSO_4$ and concentrated under reduced pressure. The crude product was purified by successive recrystallizations in CH_2Cl_2. 4-Chloro-5-hydroxymethyl-2-iodobenzaldehyde (major isomer) was obtained as a pale yellowish powder (2.377 g, 8.02 mmol, 32% over 4 steps). 2-Chloro-3-(hydroxymethyl)-6-iodobenzaldehyde (minor) **7** was obtained as a yellow powder (520 mg, 1.75 mmol, 7% over 4 steps) after filtrate concentration. TLC R_f = 0.15 (EtOAc/cyclohexane 1:4). mp: 82–83 °C. IR (ATR): 3600–2345, 1699, 1550, 1432, 1336 cm^{-1}. ^1H NMR (400 MHz, DMSO-d_6): 4.56 (2H, d, J = 6.0 Hz), 5.60 (1H, t, J = 5.6 Hz), 7.46 (1H, d, J = 8.4 Hz), 8.03 (1H, d, J = 8.4 Hz), 10.07 (1H, s). ^{13}C NMR (100 MHz, DMSO-d_6): 59.8 (CH_2), 132.3, 139.1 (CH_{arom}), 94.3, 131.9, 133.9, 141.7 (C_{arom}), 193.4 (CO). HRMS (ESI +) calcd for $C_8H_7O_2{}^{35}Cl^{127}I$ $(M+H)^+$ 296.9174, found 296.9166.

*4.1.7. 2-Chloro-3-(hydroxymethyl)-6-(2-(trimethysilyl)ethynyl) benzaldehyde (**8**)*

Under argon, $PdCl_2(PPh_3)_2$ (94.6 mg, 0.135 mmol, 2%), CuI (51.3 mg, 0.270 mmol, 4%) and trimethylsilylacetylene (2.37 mL, 11.6 mmol, 2.5 eq) were added to a solution of **7** (2.00 g, 6.74 mmol) in Et_3N (30 mL). After heating at 50 °C for 10 h, evaporation and purification by column chromatography (EtOAc/cyclohexane 3:7), compound **8** (1.04 g, 3.90 mmol, 58%) was obtained as a beige powder. TLC R_f = 0.50 (EtOAc/cyclohexane 3:7). mp: 106–108 °C. IR (ATR): 3597–3113, 1707, 1585, 1541, 1463, 1248, 1068 cm^{-1}. ^1H NMR (400 MHz, DMSO-d_6): 0.25 (9H, s), 4.61 (2H, d, J = 5.6 Hz), 5.64 (1H, t, J = 5.6 Hz), 7.63 (1H, d, J = 8.0 Hz), 7.77 (1H, d, J = 8.0 Hz), 10.47 (1H, s). ^{13}C NMR (100 MHz, DMSO-d_6): 0.4 (3 CH_3), 59.9 (CH_2), 100.9, 101.6 (C_{alkyne}), 131.3, 132.4 (CH_{arom}), 123.3, 131.6, 133.4, 142.5 (C_{arom}), 189.9 (CO). HRMS (ESI+) calcd for $C_{13}H_{16}ClO_2Si$ $(M+H)^+$ 267.0603, found 267.0595.

*4.1.8. 8-Chloro-7-(hydroxymethyl)isoquinoline (**9**)*

A solution of compound **8** (100 mg, 0.349 mmol) in ammonia in methanol (7 M, 1 mL) was irradiated for 3 × 5 min (Discover mode, Control Type Standard, P = 75 W, T = 100 °C). After solvent evaporation and purification by flash chromatography (EtOAc/cyclohexane 7:3), isoquinoline **9** (20.2 mg, 0.104 mmol, 30%) was obtained as a dark red powder. TLC R_f = 0.48 (EtOAc/cyclohexane 7:3). mp: degradation. IR (ATR): 3500–2995, 1594, 1546, 1352, 1226, 1079 cm^{-1}. ^1H NMR (400 MHz, DMSO-d_6): 4.81 (2H, d, J = 5.6 Hz), 5.65 (1H, t, J = 5.6 Hz), 7.92 (1H, dd, J_1 = 5.6 Hz, J_2 = 1.2 Hz), 7.98 (1H, d, J = 8.4 Hz), 8.02 (1H, d, J = 8.4 Hz), 8.61 (1H, d, J = 5.6 Hz), 9.58 (1H, s). ^{13}C NMR (100 MHz, DMSO-d_6): 60.3 (CH_2), 120.3, 125.8, 130.1, 143.4, 148.1 (CH_{arom}), 124.9, 135.8 (2 C_{arom}), 139.2 (C_{arom}). HRMS (ESI+) calcd for $C_{10}H_9ClNO$ $(M+H)^+$ 194.0367, found 194.0370.

*4.1.9. 8-Chloroisoquinoline-7-carbaldehyde (**10**)*

A suspension of **9** (359.5 mg, 1.862 mmol) and MnO_2 (485.7 mg, 5.587 mmol) in $CHCl_3$ (17 mL) was refluxed for 21 h. After filtration through a pad of Celite, washing with EtOAc and filtrate evaporation, the crude product was purified by flash chromatography (EtOAc/cyclohexane 1:1) Compound **10** (245.3 mg, 1.283 mmol, 69%) was obtained as a brown powder. TLC R_f = 0.70 (EtOAc/cyclohexane 7:3). mp: 135–137 °C. IR (ATR): 1686, 1614, 1544, 1440, 1347, 1224 cm^{-1}. ^1H NMR (400 MHz, DMSO-d_6): 8.03 (1H, dd, J_1 = 5.6 Hz, J_2 = 1.2 Hz), 8.11 (2H, s), 8.80 (1H, d, J = 5.6 Hz), 9.80 (1H, s), 10.62 (1H, s). ^{13}C NMR (100 MHz, DMSO-d_6): 120.6, 126.9, 127.8, 146.6, 149.4 (CH_{arom}), 125.0, 130.5, 137.5, 139.2 (C_{arom}), 189.5 (CO). HRMS (ESI+) calcd for $C_{10}H_7ClNO$ $(M+H)^+$ 192.0211, found 192.0213.

*4.1.10. Pyrido[4,3-h]quinazolin-2-amine (**11**)*

A solution of compound **10** (50.3 mg, 0.26 mmol) and guanidine carbonate (236.3 mg, 1.31 mmol, 5.2 equiv) in *N,N*-dimethylformamide (10 mL) was purged with argon for 30 min, sealed and irradiated for 45 s (Discover Mode, Control Type = Standard, P = 300 W, T = 166 °C). After cooling, the reaction was diluted with EtOAc and filtered through a pad of Celite. The organic layer was concentrated under reduced pressure. Residue was purified by flash chromatography using EtOAc, yielding the compound **11** (15.0 mg, 0.076 mmol, 30%) as a yellow powder. TLC R_f = 0.22 (EtOAc). mp: degradation. IR (ATR): 3403–2984, 2923, 1652, 1611, 1582, 1474 cm^{-1}. ^1H NMR (400 MHz, DMSO-d_6): 7.26 (2H, br s), 7.56 (1H, d, J = 8.8 Hz), 7.85 (1H, d, J = 5.6 Hz), 7.93 (1H, d, J = 8.8 Hz), 8.74 (1H, d, J = 5.6 Hz), 9.13 (1H, s), 10.08 (1H, s). ^{13}C NMR (100 MHz, DMSO-d_6): 120.1, 120.8, 129.2, 147.5, 147.8, 161.4 (CH_{arom}), 116.5, 123.1, 139.4, 151.5, 162.1 (C_{arom}). HRMS (ESI+) calcd for $C_{11}H_9N_4$ $(M+H)^+$ 197.0822, found 197.0825. HPLC: purity > 95%, t_R = 18.3 min.

4.2. In vitro kinase inhibition assays

4.2.1. Method A (^{33}P radioassay)

Kinase activities were assayed as previously described.[17,18] Only substrates used for each kinase evaluated are mentioned below.

*Hs*CDK5/p25 (human, recombinant, expressed in bacteria), substrate: histone H1.

*Ssc*CK1δ/ε (*Sus scrofa domesticus*, casein kinase 1δ/ε, affinity purified from porcine brain), peptide substrate: RRKHAAIGSpAYSITA.

*Ssc*GSK-3 α/β (*Sus scrofa domesticus*, glycogen synthase kinase-3, affinity purified from porcine brain), GS-1 peptide substrate: YRRAAVPPSPSLSRHSSPHQSpEDEEE ("Sp" stands for phosphorylated serine).

*Rn*DYRK1A-k_d (*Rattus norvegicus,* kinase domain aa 1–499, expressed in bacteria, DNA vector kindly provided by Dr. W. Becker, Aachen, Germany), peptide substrate: KKISGRLSPIMTEQ.

*Mm*CLK1 (from *Mus musculus*, recombinant, expressed in bacteria), peptide substrate: GRSRSRSRSRSR.

4.2.2. Method B (ADP-glo)

Kinase assays were carried out at 10 μM ATP in a final volume of 5 μL, following ADP-Glo protocol (Promega). The emitted luminescent signal measured using an Envision luminometer (PerkinElmer, Waltham, MA) was expressed in Relative Light Unit (RLU).

4.3. Molecular modeling experiments

After geometric optimization of compound **11** structure using Gaussian 09,[19] the docking studies were performed with AutoDock Vina.[14,15] Files for the docking were prepared from 6FT8 CLK1 structure[13] after removing of water molecules and **11** pdbqt files prepared with AutoDockTools (ADT).[20] Apolar hydrogen atoms were removed and Gasteiger charges were added. Docking experiments were performed using the default AutoDock Vina parameters.

Acknowledgements

Aurélie Job is acknowledged for HPLC analysis. W. Z., F. A., F. G. and P. M are grateful to the Auvergne Region (Jeune Chercheur Program) for funding. The French Ministry of Higher Education and Research is acknowledged for a doctoral fellowship (Y. J. E). Authors (BJ, BB, SB, SR) thank the Cancéropôle Grand Ouest (axis: natural sea products in cancer treatment), IBiSA (French Infrastructures in Life Science) and Biogenouest (Western France Life Science and Environment Core Facility Network) for supporting KISSf screening facility of USR3151 in Roscoff.

References

1. Jain P, Karthikeyan C, Moorthy NS, Waiker DK, Jain AK, Trivedi P. Human CDC2-like kinase 1 (CLK1): a novel target for Alzheimer's disease. *Curr Drug Targets.* 2014;15:539–550. https://doi.org/10.2174/1389450115666140226112321.
2. Elhady AK, Abdel-Halim M, Abadi AH, Engel M. Development of selective Clk1 and -4 inhibitors for cellular depletion of cancer-relevant proteins. *J Med Chem.* 2017;60:5377–5391. https://doi.org/10.1021/acs.jmedchem.6b01915.
3. Abbassi R, Johns TG, Kassiou M, Munoz L. DYRK1A in neurodegeneration and cancer: molecular basis and clinical implications. *Pharmacol Ther.* 2015;151:87–98. https://doi.org/10.1016/j.pharmthera.2015.03.004.
4. Esvan YJ, Zeinyeh W, Boibessot T, et al. Discovery of pyrido[3,4-*g*]quinazoline derivatives as CMCG family protein kinase inhibitors: design, synthesis, inhibitory potency and X-ray co-crystal structure. *Eur J Med Chem.* 2016;118:170–177. https://doi.org/10.1016/j.ejmech.2016.04.004.
5. Zeinyeh W, Esvan YJ, Nauton L, et al. Synthesis and preliminary in vitro kinase inhibition evaluation of new diversely substituted pyrido[3,4-*g*]quinazoline derivatives. *Bioorg Med Chem Lett.* 2016;26:4327–4329. https://doi.org/10.1016/j.bmcl.2016.07.032.
6. Tazarki H, Zeinyeh W, Esvan YJ, et al. New pyrido[3,4-*g*]quinazoline derivatives as CLK1 and DYRK1A inhibitors: synthesis, biological evaluation and binding mode analysis. *Eur J Med Chem.* 2019;166:304–317. https://doi.org/10.1016/j.ejmech.2019.01.052.
7. Echalier A, Bettayeb K, Ferandin Y, et al. Meriolins (3-(pyrimidin-4-yl)-7-azaindoles): synthesis, kinase inhibitory activity, cellular effects, and structure of a CDK2/cyclin A/meriolin complex. *J Med Chem.* 2008;51:737–751. https://doi.org/10.1021/jm700940h.
8. Wang Z, Wang C, Sun Y, Zhang N, Liu Z, Liu J. A novel strategy to the synthesis of 4-anilinoquinazoline derivatives. *Tetrahedron.* 2014;70:906–913. https://doi.org/10.1016/j.tet.2013.12.028.
9. Enthaler S, Schröder K, Inoue S, et al. Formamidines-versatile ligands for zinc-catalyzed hydrosilylation and iron-catalyzed epoxidation reactions. *Eur J Org Chem.* 2010;2010:4893–4901. https://doi.org/10.1002/ejoc.201000648.
10. Meng G, Sha YW, Zhang R, Bai N. Mild synthesis of *N′*-aryl-*N*,*N*-dimethylformamidinium chloride by Vilsmeier-Haack reagent. *Chin Chem Lett.* 2011;22:1043–1046. https://doi.org/10.1016/j.cclet.2011.03.009.
11. Zhichkin PE, Krasutsky SG, Krishnamoorthy R. *N*, N-Diisopropylformamidine (DIFA) protection of anilines in metalation reactions. *Synlett.* 2010;20:3039–3044. https://doi.org/10.1055/s-0030-1259058.
12. Billimoria AD, Cava MP. Chemistry of indolo[1,2-*c*]quinazoline: an approach to the marine alkaloid hinckdentine A. *J Org Chem.* 1994;59:6777–6782. https://doi.org/10.1021/jo00101a043.
13. Walter A, Chaikuad A, Helmer R, et al. Molecular structures of cdc2-like kinases in complex with new inhibitor chemotype. *PLoS One.* 2018;13:e0196761https://doi.org/10.1371/journal.pone.0196761.
14. Morris GM, Huey R, Lindstrom W, et al. Autodock4 and autodocktools4: automated docking with selective receptor flexibility. *J Comput Chem.* 2009;16:2785–2791. https://doi.org/10.1002/jcc.21256.
15. Trott O, Olson AJ. Autodock Vina: improving the speed and accuracy of docking with a new scoring function, efficient optimization and multithreading. *J Comput Chem.* 2010;31:455–461. https://doi.org/10.1002/jcc.21334.
16. Pettersen EF, Goddard TD, Huang CC, et al. UCSF chimera-a visualization system for exploratory research and analysis. *J Comput Chem.* 2004;25:1605–1612. https://doi.org/10.1002/jcc.20084.
17. Bach S, Knockaert M, Reinhardt J, et al. Roscovitine targets, protein kinases and pyridoxal kinase. *J Biol Chem.* 2005;280:31208–31219. https://doi.org/10.1074/jbc.M500806200.
18. Winfield HJ, Cahill MM, O'Shea KD, et al. Synthesis and anticancer activity of novel bisindolylhydrowymaleimide derivatives with potent GSK-3 kinase inhibition. *Bioorg Med Chem.* 2018;26:4209–4224. https://doi.org/10.1016/j.bmc.2018.07.012.
19. Frisch MJ, Trucks GW, Schlegel HB, Scuseria GE, Robb MA, Cheeseman JR, Scalmani G, Barone V, Mennucci B, Petersson GA, Nakatsuji H, Caricato M, Li X, Hratchian HP, Izmaylov AF, Bloino J, Zheng G, Sonnenberg JL, Hada M, Ehara M, Toyota K, Fukuda R, Hasegawa J, Ishida M, Nakajima T, Honda Y, Kitao O, Nakai H, Vreven T, Montgomery Jr JA, Peralta JE, Ogliaro F, Bearpark M, Heyd JJ, Brothers E, Kudin KN, Staroverov VN, Kobayashi R, Normand J, Raghavachari K, Rendell A, Burant JC, Iyengar SS, Tomasi J, Cossi M, Rega N, Millam MJ, Klene M, Knox JE, Cross JB, Bakken V, Adamo C, Jaramillo J, Gomperts R, Stratmann RE, Yazyev O, Austin AJ, Cammi R, Pomelli C, Ochterski JW, Martin RL, Morokuma K, Zakrzewski VG, Voth GA, Salvador P, Dannenberg JJ, Dapprich S, Daniels AD, Farkas Ö, Foresman JB, Ortiz JV, Cioslowski J, Fox DJ. *Gaussian 09, Revision D.01.* Wallingford CT: Gaussian Inc.; 2009.
20. Sanner MF. Python: a programming language for software integration and development. *J Mol Graph Mod.* 1999;17:57–61.